

Article

Six Undescribed Capnosane-Type Macrocyclic Diterpenoids from South China Sea Soft Coral *Sarcophyton crassocaule*: Structural Determination and Biological Evaluation

Hanyang Peng^{1,2,†}, Yanbo Zeng^{1,3,*,†} , Hao Wang¹ , Wenjun Chang^{1,3}, Huiqin Chen¹, Fengjuan Zhou², Haofu Dai^{1,*} and Xiachang Wang^{2,*} 

- ¹ Hainan Provincial Key Laboratory for Functional Components Research and Utilization of Marine Bio-Resources, Institute of Tropical Bioscience and Biotechnology, Chinese Academy of Tropical Agricultural Sciences & Key Laboratory for Biology and Genetic Resources of Tropical Crops of Hainan Province, Hainan Institute for Tropical Agricultural Resources, Haikou 571101, China; 17379935106@163.com (H.P.); wanghao@itbb.org.cn (H.W.); changwenjun@itbb.org.cn (W.C.); chenhuiqin@itbb.org.cn (H.C.)
- ² Jiangsu Key Laboratory for Functional Substances of Chinese Medicine, Nanjing University of Chinese Medicine, Nanjing 210023, China; 20210662@njucm.edu.cn
- ³ Zhanjiang Experimental Station of Chinese Academy of Tropical Agricultural Sciences, Zhanjiang 524013, China
- * Correspondence: zengyanbo@itbb.org.cn (Y.Z.); daihaofu@itbb.org.cn (H.D.); xiachangwang@njucm.edu.cn (X.W.)
- † These authors contributed equally to this work.

Abstract: Six undescribed capnosane-type macrocyclic diterpenes sarcocrassolins A–F (1–6) and one related known analog pavidolide D (7) were isolated from *Sarcophyton crassocaule*, a soft coral collected off the Nansha Islands, in the South China Sea. Their complete structures, relative configurations and absolute configurations were established through comprehensive spectroscopic analysis, quantum mechanical nuclear magnetic resonance (QM-NMR) and single-crystal X-ray diffraction. Sarcocrassolins D (4) and E (5) showed inhibitory activity against lipopolysaccharide (LPS)-stimulated inflammatory responses in RAW264.7 cells with IC₅₀ values of 76.8 ± 8.0 μM and 93.0 ± 3.8 μM, respectively.

Keywords: soft coral; *Sarcophyton crassocaule*; cembranoids; capnosane-type macrocyclic diterpenes; absolute configuration; anti-inflammation



Citation: Peng, H.; Zeng, Y.; Wang, H.; Chang, W.; Chen, H.; Zhou, F.; Dai, H.; Wang, X. Six Undescribed Capnosane-Type Macrocyclic Diterpenoids from South China Sea Soft Coral *Sarcophyton crassocaule*: Structural Determination and Biological Evaluation. *Mar. Drugs* **2023**, *21*, 645. <https://doi.org/10.3390/md21120645>

Academic Editor: Eva Zubia

Received: 16 November 2023

Revised: 12 December 2023

Accepted: 13 December 2023

Published: 18 December 2023



Copyright: © 2023 by the authors. Licensee MDPI, Basel, Switzerland. This article is an open access article distributed under the terms and conditions of the Creative Commons Attribution (CC BY) license (<https://creativecommons.org/licenses/by/4.0/>).

1. Introduction

Cembranoids are a large family of diterpenoids having a highly flexible 14-membered macrocyclic skeleton, which is generated from geranylgeranyl diphosphate (GGPP) by head-to-tail cyclization [1]. The first cembranoid, named cembrene, was isolated from the oleoresin of the white bark pine in 1962 [2]. Afterward, plenty of cembranoids have been isolated from plants, insects or marine organisms. The capnosane-type macrocyclic diterpenes, which have a 5/11-fused bicyclic carbon skeleton, are thought to be biogenetically produced from cembranoids via transannular cyclization between the C-3 and C-7 positions or ring rearrangement [3–5]. Capnosane-type macrocyclic diterpenes are rarely encountered. Hitherto, only 48 capnosane-type macrocyclic diterpenes have been reported from 14 species of soft corals (including *Sarcophyton boettgeri* [3], *Sarcophyton trocheliophorum* [6–9], *Klyxum flaccidum* [10], *Sinularia rigida* [11], *Sinularia polydactyla* [12], *Sarcophyton mililatensis* [13], *Sinularia pavida* [14], *Sarcophyton elegans* [15], *Lobophytum* sp. [16], *Sarcophyton solidun* [17], *Cespitularia* sp. [18], *Alcyonium coralloides* [19], *Lobophytum pauciflorum* [20], and *Sinularia humilis* [21]). Moreover, these capnosane-type macrocyclic diterpenes have been proved to possess a wide variety of biological activities, including anticancer [10,15], anti-inflammatory [3,20] and inhibition of tyrosine protein phosphatase 1B [8,12].

Soft corals of genus *Sarcophyton* are widely distributed in shallow waters of the Mediterranean Sea, Red Sea, Arctic and Indo-Pacific region [22]. Besides, the genus *Sarcophyton*, which includes many species, is a rich source of bioactive natural metabolites. Most of these species of the genus *Sarcophyton* have undergone thorough chemical investigations [23], including the species *Sarcophyton crassocaule*. Despite the fact that many diterpenoids were isolated from *S. crassocaule*, capnosane-type macrocyclic diterpenes have not been encountered. In our continuous search for pharmaceutical leads from structurally diverse secondary metabolites of soft corals [24], six undescribed capnosane-type macrocyclic diterpenes named sarcocrassolins A–F (1–6) and one related known analogue, pavidolide D (7), (Figure 1) were isolated from *S. crassocaule*, a soft coral collected off the Nansha Islands. This is the first report of capnosane-type macrocyclic diterpenes in the soft coral *S. crassocaule*. Herein, we discuss the isolation, structural elucidation, biological activity and plausible biosynthetic pathway of these capnosane-type macrocyclic diterpenes.

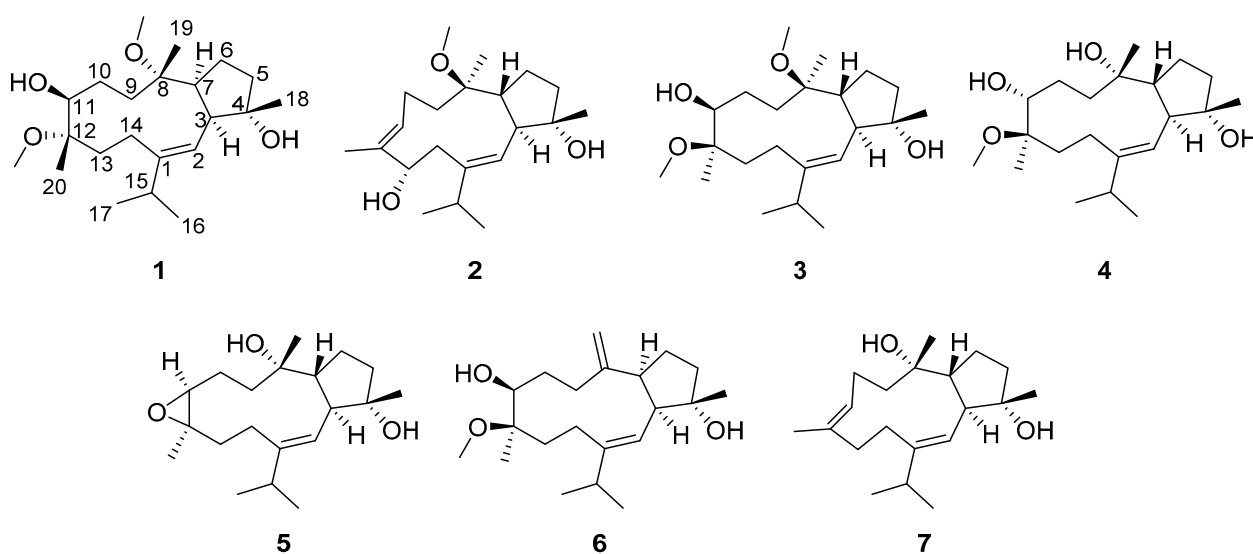


Figure 1. Structures of compounds 1–7 from the soft coral *Sarcophyton crassocaule*.

2. Results and Discussion

2.1. Structure Elucidation of New Compounds 1–6

Sarcocrassolin A (1) was isolated as a white powder. The HRESIMS data at m/z 391.2820 (calculated as 391.2819 for $C_{22}H_{40}O_4Na$, $[M + Na]^+$) revealed the molecular formula of 1 to be $C_{22}H_{40}O_4$ with three indexes of hydrogen deficit, which was validated by the ^{13}C NMR and DEPT data. The presence of hydroxy and olefinic groups was suggested by the IR absorption bands at 3418 and 1638 cm^{-1} , respectively. Five methyl groups (δ_H 0.99, 1.07, 1.08, 1.10, 1.26), two methoxy groups (δ_H 3.19, 3.22), one oxymethine (δ_H 3.59) and one olefinic proton (δ_H 5.02) were detected in the 1H NMR spectrum of 1 (Table 1). The ^{13}C NMR spectrum revealed twenty-two carbon signals, including four quaternary carbons (δ_C 146.7, 83.2, 79.4, 79.3), five methines (δ_C 121.0, 78.7, 52.0, 50.0, 32.8), six methylenes (δ_C 37.5, 23.1, 35.7, 25.1, 33.2, 21.3), five methyls (δ_C 21.6, 23.1, 26.5, 19.2, 19.1) and two methoxy groups (δ_C 48.1, 49.5) (Table 2). A double bond in 1 accounted for one degree of unsaturation and indicated that the structure had two rings as a result of the remaining two indexes of hydrogen deficit. Because 1 and pavidolide D (7) were co-isolated secondary metabolites, their similar NMR data suggested that 1 was most likely a diterpene of the capnosane-type. Following that, the planar structure of 1 was ascertained by the 1H - 1H COSY and HMBC spectra. First of all, four fragments a–d (Figure 2) were established by comprehensive analysis of the 1H - 1H COSY correlations of H₃-16 (δ_H 1.08)/H-15 (δ_H 2.23)/H₃-17 (δ_H 0.99) (a), H-2 (δ_H 5.02)/H-3 (δ_H 2.49)/H-7 (δ_H 2.88)/H₂-6 (δ_H 1.86, 1.75)/H₂-5 (δ_H 1.77, 1.66) (b), H₂-9 (δ_H 1.97, 1.62)/H₂-10 (δ_H 1.56, 1.32)/H-11 (δ_H 3.59) (c) and H₂-13 (δ_H 2.15, 1.19)/H₂-14 (δ_H 2.09, 1.97) (d). The HMBC

cross peaks from H-2 (δ_{H} 5.02) to C-1 (δ_{C} 146.7)/C-14 (δ_{C} 21.3), and from H₃-16 (δ_{H} 1.08), H₃-17 (δ_{H} 0.99) to C-1 (δ_{C} 146.7)/C-15 (δ_{C} 32.8) determined that fragments **a**, **b** and **d** were linked via C-1. The presence of a cyclopentane was demonstrated by the HMBC cross peaks from H₃-18 (δ_{H} 1.10) to C-3 (δ_{C} 52.0)/C-4 (δ_{C} 83.2)/C-5 (δ_{C} 37.5) as well as from H-3 (δ_{H} 2.49) to C-5 (δ_{C} 37.5)/C-6 (δ_{C} 23.1). The fragments **b** and **c** were found to be linked via C-8, whereas fragments **c** and **d** via C-12, according to the HMBC cross peaks from H₃-19 (δ_{H} 1.07) to C-7 (δ_{C} 50.0)/C-8 (δ_{C} 79.3)/C-9 (δ_{C} 35.7) and from H₃-20 (δ_{H} 1.26) to C-11 (δ_{C} 78.7)/C-12 (δ_{C} 79.4)/C-13 (δ_{C} 33.2). Finally, the HMBC cross peaks from 8-OMe (δ_{H} 3.19) to C-8 (δ_{C} 79.3) and from 12-OMe (δ_{H} 3.22) to C-12 (δ_{C} 79.4) were utilized to infer the position of two methoxy groups, one at C-8 and the other at C-12. Thus, as can be seen in Figure 1, the complete planar structure of **1** was determined.

Table 1. ¹H NMR data for compounds 1–6 (500 MHz, CDCl₃).

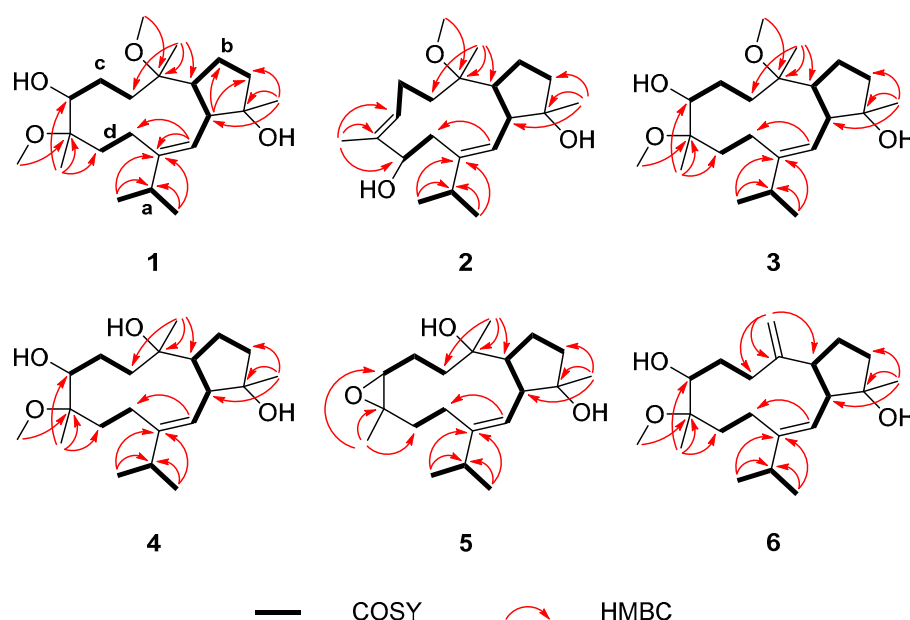
No.	1	2	3	4	5	6
2	5.02 d (11.7)	5.00 d (9.3)	5.16 d (10.3)	5.21 d (10.4)	5.31 d (12.0)	4.88 d (10.7)
3	2.49 dd (11.7, 5.3)	2.34 t (9.3)	2.36 dd (11.5, 10.3)	2.41 t (10.9)	2.97 t (11.5)	2.41 dd (10.7, 5.9)
5	1.77 m	1.58–1.66 m	1.74 m	1.74 m	1.79 m	1.79 m
	1.66 m		1.69 m			1.69 m
6	1.86 m	1.59 m	1.68 m	1.72 m	1.97 m	1.85–1.95 m
	1.75 m	1.48 m	1.48 m	1.50 m	1.72 m	
7	2.88 m	2.15 m	1.97 m	1.93 m	2.73 m	2.17 m
9	1.97 m	2.00 m	1.74 m	1.69 m	1.99 m	2.27 m
	1.62 m	1.55 m	1.58 ddd (15.5, 6.7, 2.2)		1.73 m	2.16 m
10	1.56 m	2.08–2.19 m	1.90 m	1.67 m	2.14 m	1.58 m
	1.32 m		1.30 m	1.41 m	1.22 m	1.45 m
11	3.59 t (11.0)	5.38 t (7.7)	3.66 t (10.1)	3.68 t (9.5)	3.16 dd (10.0, 4.3)	3.60 t (9.3)
13	2.15 m	3.97 dd (11.0, 2.2)	2.10 m	2.14 m	2.07 m	2.09 m
	1.19 m		1.21 m	1.24 m	1.72 m	1.15 m
14	2.09 m	2.81 t (11.9)	2.13 m	2.18 m	2.60 td (13.3, 6.3)	1.99 m
	1.97 m	1.98 m	1.94 m	2.00 m	1.97 m	1.89 m
15	2.23 m	2.26 sept (6.8)	2.22 m	2.28 m	2.37 sept (6.8)	2.22 m
16	1.08 d (6.8)	1.08 d (6.8)	1.10 d (6.8)	1.11 d (6.8)	1.14 d (6.8)	1.06 d (6.8)
17	0.99 d (6.8)	1.07 d (6.8)	1.02 d (6.8)	1.05 d (6.8)	1.05 d (6.8)	0.98 d (6.8)
18	1.10 s	1.06 s	1.06 s	1.08 s	1.16 s	1.14 s
19	1.07 s	1.15 s	1.08 s	1.16 s	1.24 s	5.12 br s
20	1.26 s	1.69 s	1.25 s	1.27 s	1.17 s	4.89 br s
8-OMe	3.19 s	3.12 s	3.10 s			1.24 s
12-OMe	3.22 s		3.20 s	3.21 s		3.21 s

Table 2. ¹³C NMR data for compounds 1–6 (125 MHz, CDCl₃).

No.	1	2	3	4	5	6
1	146.7, C	141.6, C	146.8, C	151.0, C	146.5, C	146.6, C
2	121.0, CH	127.2, CH	122.7, CH	121.4, CH	120.4, CH	123.0, CH
3	52.0, CH	50.0, CH	51.6, CH	51.7, CH	50.0, CH	56.9, CH
4	83.2, C	82.4, C	81.4, C	81.6, C	82.2, C	82.6, C
5	37.5, CH ₂	39.5, CH ₂	37.7, CH ₂	38.4, CH ₂	39.6, CH ₂	40.7, CH ₂
6	23.1, CH ₂	24.8, CH ₂	24.7, CH ₂	25.0, CH ₂	25.3, CH ₂	31.7, CH ₂
7	50.0, CH	51.0, CH	52.7, CH	55.7, CH	48.5, CH	51.5, CH
8	79.3, C	78.0, C	80.0, C	75.8, C	74.5, C	154.3, C
9	35.7, CH ₂	36.2, CH ₂	30.4, CH ₂	33.4, CH ₂	39.2, CH ₂	34.2, CH ₂
10	25.1, CH ₂	23.0, CH ₂	24.9, CH ₂	25.6, CH ₂	23.4, CH ₂	28.8, CH ₂

Table 2. Cont.

No.	1	2	3	4	5	6
11	78.7, CH	127.9, CH	78.9, CH	78.4, CH	61.7, CH	74.3, CH
12	79.4, C	134.3, C	79.4, C	79.3, C	60.1, C	79.7, C
13	33.2, CH ₂	76.2, CH	33.7, CH ₂	33.7, CH ₂	33.9, CH ₂	33.5, CH ₂
14	21.3, CH ₂	38.3, CH ₂	21.6, CH ₂	21.7, CH ₂	25.0, CH ₂	21.9, CH ₂
15	32.8, CH	34.5, CH	32.9, CH	33.0, CH	31.3, CH	32.1, CH
16	21.6, CH ₃	22.2, CH ₃	22.1, CH ₃	22.1, CH ₃	20.2, CH ₃	21.8, CH ₃
17	23.1, CH ₃	24.3, CH ₃	24.0, CH ₃	23.8, CH ₃	24.4, CH ₃	23.4, CH ₃
18	26.5, CH ₃	24.9, CH ₃	24.9, CH ₃	24.9, CH ₃	24.3, CH ₃	25.1, CH ₃
19	19.2, CH ₃	24.9, CH ₃	24.1, CH ₃	30.2, CH ₃	25.9, CH ₃	111.5, CH ₂
20	19.1, CH ₃	11.7, CH ₃	19.0, CH ₃	19.0, CH ₃	20.9, CH ₃	19.0, CH ₃
8-OMe	48.1, CH ₃	48.8, CH ₃	49.4, CH ₃			
12-OMe	49.5, CH ₃		49.5, CH ₃	49.5, CH ₃		49.5, CH ₃

Figure 2. ¹H–¹H COSY and key HMBC correlations of compounds 1–6.

The significant ROESY cross peaks between H-2 (δ_{H} 5.02) and H₃-16 (δ_{H} 1.08) indicated the double-bond Δ^1 in **1** in *E*-geometry. The ROESY cross peaks between H-3 (δ_{H} 2.49)/H-7 (δ_{H} 2.88), H-2 (δ_{H} 5.02)/H₃-18 (δ_{H} 1.10), H-2 (δ_{H} 5.02)/H₃-19 (δ_{H} 1.07) and the absence of ROESY correlation between H-3 (δ_{H} 2.49)/H₃-18 (δ_{H} 1.10), H-2 (δ_{H} 5.02)/H-7 (δ_{H} 2.88), H-2 (δ_{H} 5.02)/H-3 (δ_{H} 2.49) indicated that H-3 and H-7 were at the same side and arbitrarily assigned as being in α -configuration, whereas H₃-18 and H₃-19 were assigned as being in β -configuration (Figure 3). The ROESY experiment did not allow for determining the relative configuration of C-8, C-11 and C-12 due to the presence of a highly flexible macrocycle. As a result, QM-NMR employing DP4+ probability analysis was carried out. This is a potent tool whose application for capnosane-type diterpenes has been proven to be reliable [3]. QM-NMR calculations on eight potential isomers **1a–1h** (Figure 4) were then performed. According to the experimental results, the NMR data of compound **1** offered the highest degree of matching for **1g** (3S*, 4S*, 7S*, 8S*, 11S*, 12S*) (DP4+ probability 99.81%). Therefore, the 8S* configuration was consistent with the correlations observed in the ROESY spectrum. Finally, the structure of compound **1** was determined by the analysis presented above and represented in Figure 1.

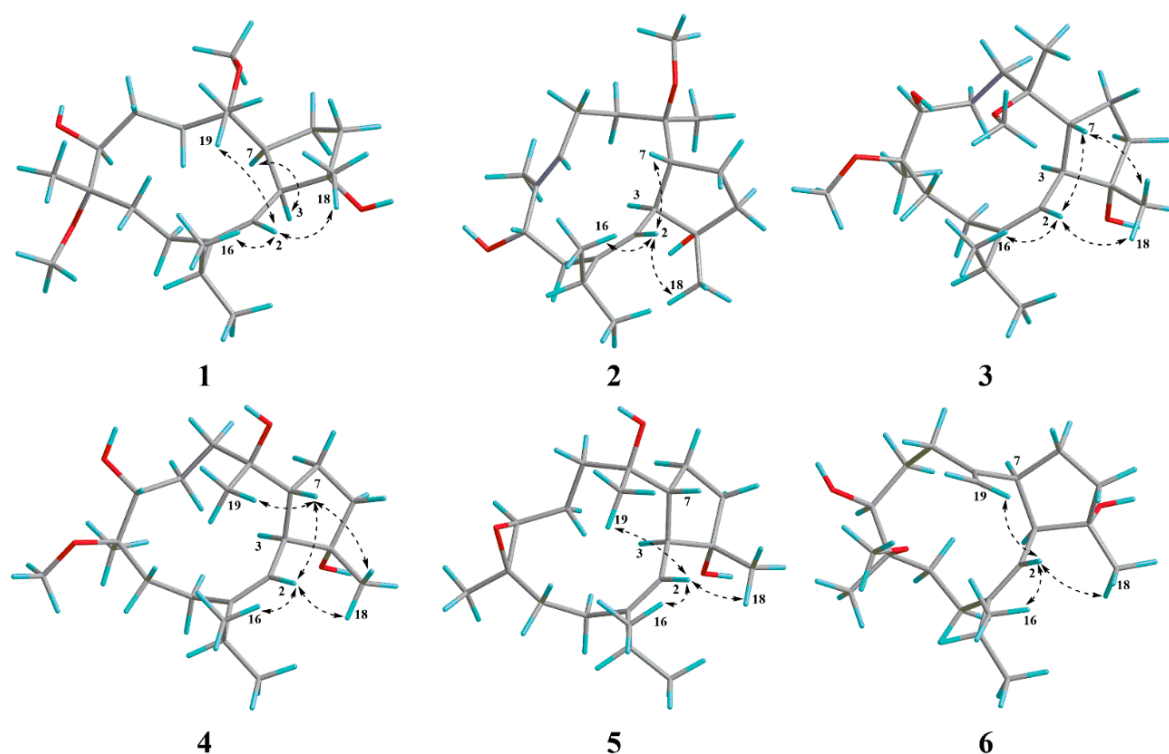


Figure 3. Key ROESY correlations of compounds 1–6.

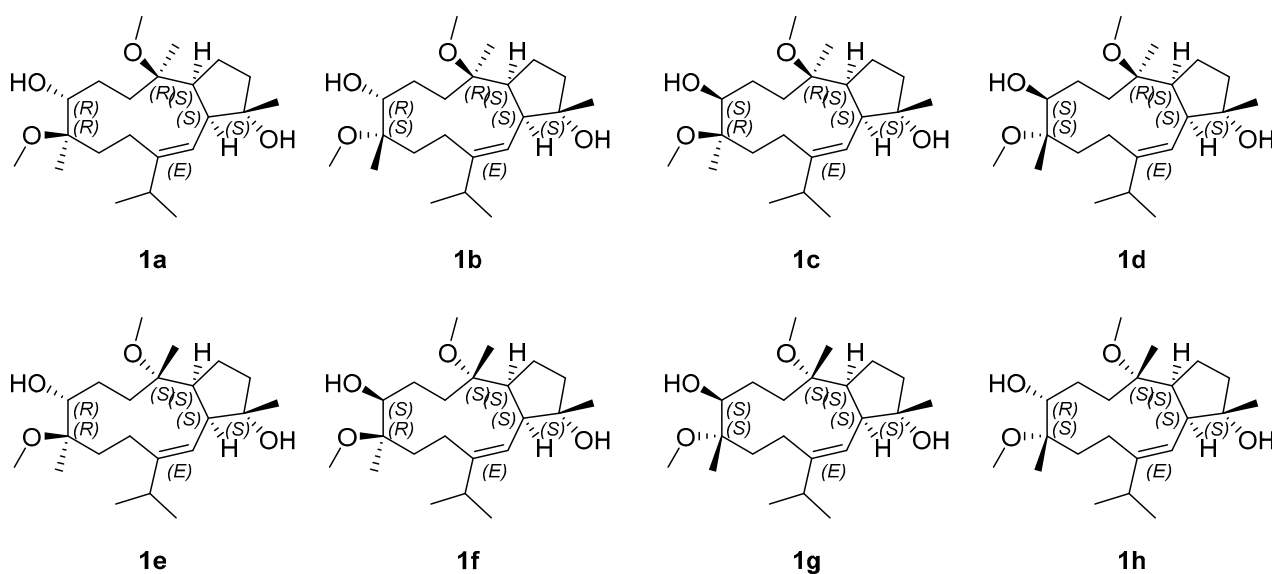


Figure 4. Structures of isomers of compound 1.

Sarcocrassin B (**2**), isolated as a colorless crystal, had a molecular formula of $C_{21}H_{36}O_3$ according to its HRESIMS data at m/z 695.5211 (calculated as 695.5221 for $C_{42}H_{72}O_6Na$, $[2M + Na]^+$), with four degrees of unsaturation. Additionally, the characteristic infrared absorption bands at 3421 and 1602 cm^{-1} provided evidence for the presence of hydroxyl and olefinic groups. The 1H NMR data revealed the signals of five methyl groups (δ_H 1.06, 1.07, 1.08, 1.15, 1.69), one methoxy group (δ_H 3.12) and two olefinic protons (δ_H 5.00, 5.38). The ^{13}C NMR data showed the presence of 21 signals, which comprised two pairs of olefinic carbons, five methyl signals, five methylene signals, four sp^3 methines, two sp^3 quaternary carbons and one methoxy carbon. Based on a comprehensive analysis of its NMR spectra, compound **2** almost resembled trocheliophol G, a capnosane-type

macrocyclic diterpene from *S. trocheliophorum* [6]. The major difference was observed at the C-13 and C-14 positions, where a hydroxy at the C-13 position in **2** shifted to the C-14 position in trocheliophol G. The significant HMBC cross peaks from H₃-20 (δ_{H} 1.69) to C-11 (δ_{C} 127.9)/C-12 (δ_{C} 134.3)/C-13 (δ_{C} 76.2), and from H-2 (δ_{H} 5.00) to C-14 (δ_{C} 38.3) as well as the ^1H - ^1H COSY cross peaks of H-13 (δ_{H} 3.97)/H-14a (δ_{H} 1.97) and H-13 (δ_{H} 3.97)/H-14b (δ_{H} 2.80), further supported this conclusion. The ROESY spectrum verified the *E* configurations of the double-bonds Δ^1 and Δ^{11} , with the essential cross peaks of H-2 (δ_{H} 5.00)/H₃-16 (δ_{H} 1.08) and the lack of H-11 (δ_{H} 5.38)/H₃-20 (δ_{H} 1.69). In addition, the key ROESY cross peaks of H-2 (δ_{H} 5.00)/H₃-18 (δ_{H} 1.06) and H-2 (δ_{H} 5.00)/H-7 (δ_{H} 2.15), along with the lack of cross peak of H-2 (δ_{H} 5.00)/H-3 (δ_{H} 2.34) indicated that H-7 and H₃-18 were co-facial, while H-3 was on the opposite side of the molecule (Figure 3). The relative configuration of C-8 and C-13 could not be established from the ROESY experiment either. However, an appropriate single crystal of compound **2** was obtained in a solution of MeOH/H₂O (20:1). Ultimately, as shown in Figure 5, the absolute configuration of **2** was obtained by analyzing the X-ray crystallographic data (Flack parameter: $-0.3(4)$) and was unambiguously established as 3*S*, 4*S*, 7*R*, 8*R*, 13*S*.

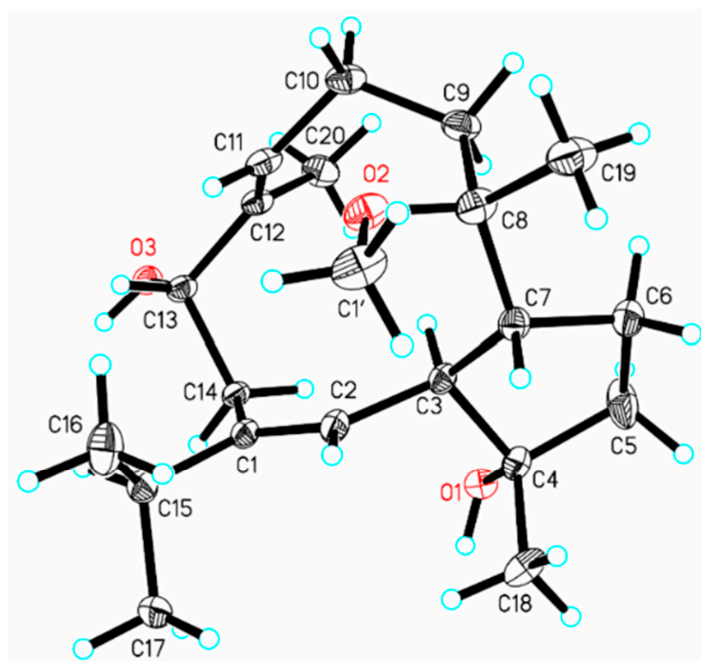


Figure 5. Single-crystal X-ray structure of **2** (the ellipsoids are shown at a 30% probability level).

Sarcocrassolin C (**3**) was isolated as a colorless oil and assigned the molecular formula $\text{C}_{22}\text{H}_{40}\text{O}_4$, identical to that of **1**, according to the HRESIMS ion peak at m/z 391.2819 (calculated as 391.2819 for $\text{C}_{22}\text{H}_{40}\text{O}_4\text{Na}$, $[\text{M} + \text{Na}]^+$), with three degrees of unsaturation. The characteristic infrared absorption bands at 3431 and 1632 cm^{-1} indicated the presence of hydroxy and olefinic groups, respectively. By comparing the ^1H NMR and ^{13}C NMR data of compounds **3** and **1**, we found that compound **3** was highly similar to **1**. Following that, the analysis of NMR data of compound **3** implied that compounds **3** and **1** shared the same planar structure. The main difference was that H-7 upfield-shifted significantly from δ_{H} 2.88 in **1** to δ_{H} 1.97 in **3**. Meanwhile, the higher value of $J_{\text{H-3/H-7}}$ (11.5 Hz) in **3** compared to $J_{\text{H-3/H-7}}$ (5.3 Hz) in **1** indicated that **3** and **1** exhibited different configurations at C-7. The ROESY cross peak between H-7 (δ_{H} 1.97) and H₃-18 (δ_{H} 1.06) together with the lack of ROESY correlation between H-3 (δ_{H} 2.36) and H-7 (δ_{H} 1.97) also validated this hypothesis. The double-bond Δ^1 in **3** possessed *E*-geometry, according to the ROESY cross peaks between H-2 (δ_{H} 5.16) and H₃-16 (δ_{H} 1.10). The correlations of H-2 (δ_{H} 5.16)/H₃-18 (δ_{H} 1.06) and H-2 (δ_{H} 5.16)/H-7 (δ_{H} 1.97) showed in ROESY spectrum, whereas no cross peaks of H-3 (δ_{H} 2.36)/H₃-18 (δ_{H} 1.06) and H-2 (δ_{H} 5.16)/H-3 (δ_{H} 2.36) were observed (Figure 3).

This indicated that H₃-18 and H-7 were co-facial, whereas H-3 was on the opposite side of the molecule. The identical key ROESY correlations between compounds **3** and **2** indicated that the relative configuration of C-3, C-4 and C-7 in compounds **3** and **2** could be the same and established as 3*S**, 4*S**, 7*R**, which was unambiguously defined by single-crystal X-ray diffraction in compound **2**. The ROESY experiment also failed to identify the relative configuration of C-8, C-11 and C-12. Therefore, eight potential isomers **3a–3h** (Figure S57) were calculated. The correlation coefficient $R^2 = 0.9981$ (DP4+ probability, 100%) indicated that the experimental NMR results of **3** were more consistent with **3c** (3*S**, 4*S**, 7*R**, 8*R**, 11*S**, 12*R**) than other isomers. Consequently, the relative configuration of **3** ended up being established as illustrated in Figure 1.

Sarcocrassolin D (**4**) was obtained as a colorless oil. Its molecular formula was established as C₂₁H₃₈O₄ by HRESIMS data at m/z 731.5432 (calculated as 731.5432 for C₄₂H₇₆O₈Na, [2M + Na]⁺). The analysis of the NMR data of **4** showed that **4** mostly resembled **3**. The major difference between **4** and **3** was at the C-8 position, where the methoxy group in **3** was substituted by a hydroxy group in **4**. This alteration was further validated by their 14-mass unit difference. The double-bond Δ^1 in **4** was proposed to have *E*-geometry, in accordance with the ROESY cross peak between H-2 (δ_H 5.21) and H₃-16 (δ_H 1.11). Furthermore, the relative configuration of C-3, C-4 and C-7 could be tentatively established as 3*S**, 4*S** and 7*R**, respectively, based on the similar crucial ROESY correlation between **3** and **4** (Figure 3). Finally, eight potential isomers **4a–4h** (Figure S58) were calculated to explicate the spatial arrangement of C-11, C-12 and C-8. The correlation coefficient $R^2 = 0.9835$ (DP4+ probability, 100%) suggested that **4e** (3*S**, 4*S**, 7*R**, 8*S**, 11*R**, 12*R**) was more compatible with the experimental NMR results. Consequently, the relative configuration of **4** was defined as shown in Figure 1.

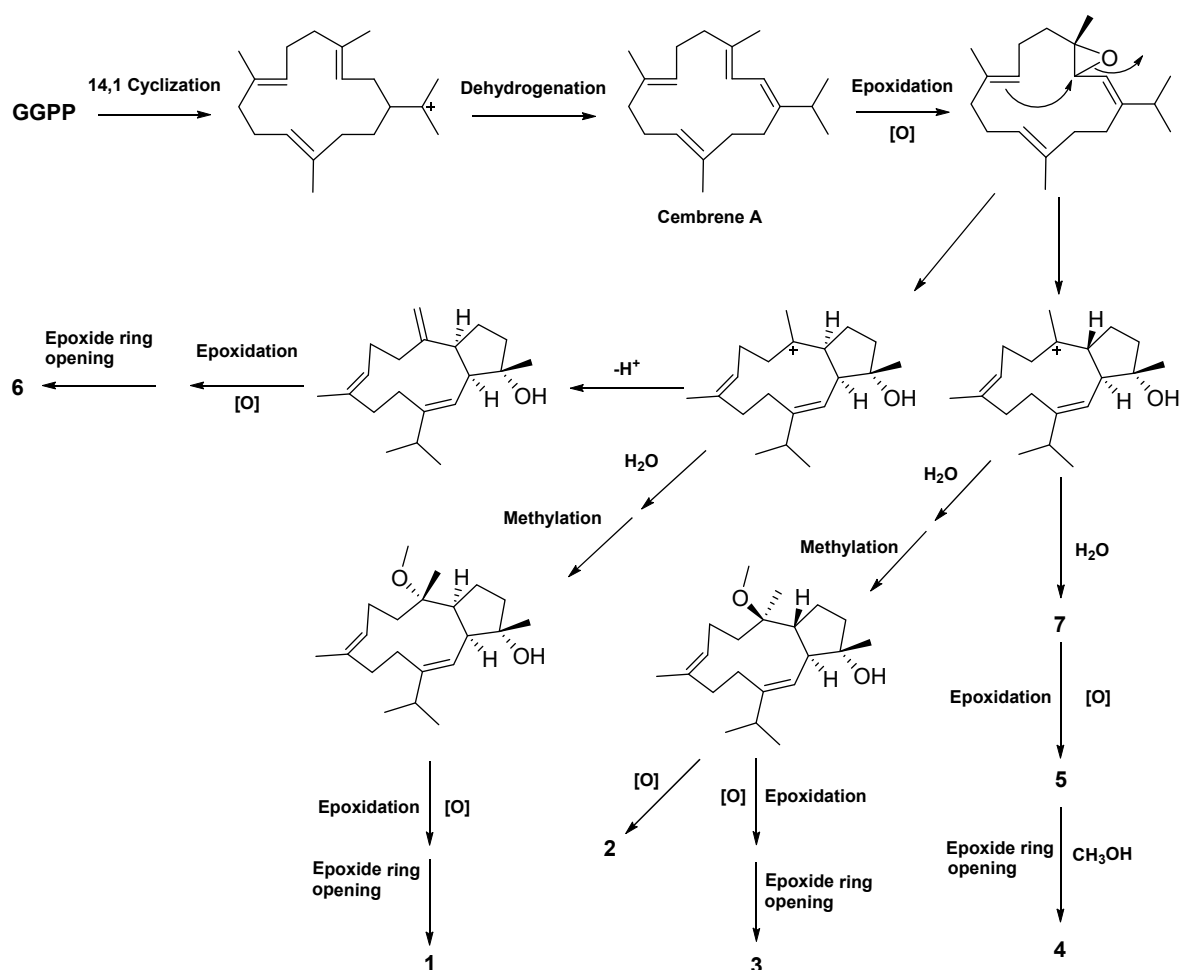
The HRESIMS ion peak at m/z 345.2398 (calculated as 345.2400 for C₂₀H₃₄O₃Na, [M + Na]⁺) revealed the molecular formula of sarcocrassolin E (**5**) to be C₂₀H₃₄O₃ with four indexes of hydrogen deficit. The existence of hydroxy and olefinic groups could be determined by the characteristic infrared absorption bands at 3393 and 1650 cm⁻¹, respectively. The ¹³C NMR spectrum revealed twenty carbon signals, which were classified by DEPT and HSQC spectra and then attributed to four quaternary carbons, five methines, six methylenes and five methyls. One double bond and one epoxy ring were composed of two methines, C-2 (δ_C 120.4, δ_H 5.31) and C-11 (δ_C 61.7, δ_H 3.16), as well as two quaternary carbons, C-1 (δ_C 146.5) and C-12 (δ_C 60.1), which contributed to the two indexes of hydrogen deficit. The remaining two indexes of hydrogen deficit thus revealed that the molecule contained two rings. Following that, the entire planar structure of **5** could be constructed using the 2D NMR data as depicted in Figure 2. When the NMR data were further analyzed, it became clear that compound **5** and sarcophytrol B [7], a capnosane-type macrocyclic diterpene that had previously been identified, were highly similar. The major difference was the configuration of double-bond Δ^1 . In fact, that had an *E* configuration in **5** and *Z* configuration in sarcophytrol B, which was established by the ROESY cross peaks between H-2 and H₃-16 in compound **5**. It was also possible to establish the relative configurations of C-3, C-4 and C-7 as 3*S**, 4*S** and 7*R**, respectively, by the similar key ROESY cross peaks observed in compounds **4** and **5**. Consequently, four possible isomers **5a–5d** (Figure S59) were calculated. Based on the experimental results, the NMR data of compound **5** provided the highest degree of matching for **5d** (3*S**, 4*S**, 7*R**, 8*S**, 11*S**, 12*R**), with 100% probabilities. Consequently, the relative configuration of **5** was defined as 3*S**, 4*S**, 7*R**, 8*S**, 11*S** and 12*R** (Figure 1).

Sarcocrassolin F (**6**), isolated as a colorless oil, had a molecular formula C₂₁H₃₆O₃ based on the HRESIMS data at m/z 359.2557 (calculated as 359.2557 for C₂₁H₃₆O₃Na, [M + Na]⁺). The analysis of its ¹H and ¹³C NMR spectral characteristics data showed that **6** displayed extensive resemblance to **1**, except for the existence of an exocyclic double bond at C-8, C-19 in **6** instead of a methoxy and a methyl at C-8 in **1**, which was validated by key HMBC cross peaks from H-19 to C-7/C-8/C-9. According to the noticeable ROESY cross peak of H-2/H₃-16, the double-bond Δ^1 in **6** was proven to be of the *E*-geometry. The

ROESY cross peak between H-2 and H₃-18, along with the lack of cross peaks of H-2/H-3 and H-3/H₃-18, indicated that H-3 and H₃-18 were oriented on the opposite side of the molecule. Due to the insufficient signals, ROESY correlations were unable to ascertain the relative configuration of C-7. However, the nearly identical coupling constant of $J_{H-3/H-7}$ (5.9 Hz) in **6** and $J_{H-3/H-7}$ (5.3 Hz) in **1** revealed that H-3 and H-7 had the same orientation in both molecules. Finally, the QM-NMR using DP4+ probability analysis was carried out for the four potential isomers **6a–6d** (Figure S60) to explicate the spatial arrangement of C-11 and C-12. The experimental data indicated that **6d** (3*S**, 4*S**, 7*S**, 11*S**, 12*R**) was more consistent with the correlation coefficient $R^2 = 0.9975$ (DP4 + probability, 100%). Consequently, the relative configuration of **6** was depicted as drawn in Figure 1.

Compound **7** was identified as pavidolide D on the basis of the MS and NMR data analyses and comparison with the NMR data from a previously reported article [14].

Because all compounds **1–7** possessed the same 5/11-fused bicyclic carbon skeleton and were obtained from the same animal material, it was reasonable to assume that they originated from the same biosynthetic pathway. According to their structural characteristics, a potential biosynthetic pathway of compounds **1–7** has been postulated (Scheme 1). The precursor geranylgeranyl diphosphate (GGPP) via 14,1 cyclization and dehydrogenation generates intermediate cembrene A. Subsequently, the 5/11-fused bicyclic carbon skeleton was generated by epoxidation and transannular cyclization from cembrene A. Finally, all compounds **1–7** were obtained after undergoing a series of reactions (such as methylation, epoxidation and dehydrogenation).



Scheme 1. Postulated biosynthetic pathway of compounds **1–7**.

2.2. In Vitro Biological Assay

In biological assays, all the abovementioned compounds were tested for their cytotoxic and anti-inflammatory activities. In cytotoxicity screening assay, all compounds were assayed against five cell lines: SGC-7901 (human gastric cells), K562 (human myeloid leukemia cells), BEL-7402 (human hepatocellular carcinoma cells), HeLa (human cervical carcinoma cells) and A549 (human lung cancer cells). Unfortunately, none of these compounds displayed obvious cytotoxic activity at a concentration of 20.0 $\mu\text{g}/\text{mL}$. In anti-inflammatory testing, compounds **4** and **5** exhibited weak inhibitory activity of NO release in LPS-stimulated RAW264.7 cells, with the IC_{50} values of $76.8 \pm 8.0 \mu\text{M}$ and $93.0 \pm 3.8 \mu\text{M}$, respectively (Table 3). The positive control used was quercetin, which had an IC_{50} value of $12.7 \pm 2.4 \mu\text{M}$. The cell viability of RAW264.7 cells upon treatment with the compounds was also determined by the MTT method, and the result indicated that compounds **3** and **4** had no cytotoxicity against RAW264.7 cells at a concentration of 100.0 μM .

Table 3. Anti-inflammatory effect of compounds 1–7.

Compounds	$\text{IC}_{50} \pm \text{SD} (\mu\text{M})$	Compounds	$\text{IC}_{50} \pm \text{SD} (\mu\text{M})$
1	>100	5	93.0 ± 3.8
2	>100	6	>100
3	>100	7	>100
4	76.8 ± 8.0	Quercetin	12.7 ± 2.4

3. Materials and Methods

3.1. General Experimental Procedures

Optical rotation was performed on a Modular Circular Polarimeter (Anton Paar, Graz, Austria). The IR spectra were recorded on a Nicolet 380 infrared spectrometer (Thermo Electron Corporation, Madison, WI, USA). UV and CD data were collected on a MOS-500 spectrometer (Biologic, Seyssinet-Pariset, France). NMR spectra were obtained on a Bruker AV-500 NMR spectrometer (Bruker, Bremen, Germany), using the TMS as an internal standard. HRESIMS spectra were measured on an API QSTAR Pulsar mass spectrometer (Bruker, Bremen, Germany). Analytical HPLC was recorded on an Agilent Technologies 1260 Infinity II with an Agilent DAD G1315D detector (Agilent, Palo Alto, CA, USA). Semi-preparative HPLC was performed on an ODS column (COSMOSIL-packed C_{18} , 5 mm, 10 mm \times 250 mm). Column chromatography was performed on a Sephadex LH-20 (Merck, Darmstadt, Germany) and Silica gel (60–80, 200–300 and 300–400 mesh, Qingdao Marine Chemical Co., Ltd., Qingdao, China). Analytical TLC was conducted on precoated silica gel GF254 plates (Qingdao Marine Chemical Co., Ltd., Qingdao, China), and the spots were detected by spraying with 10% H_2SO_4 in EtOH and subsequent heating.

3.2. Animal Materials

The soft coral *S. crassocaule* was collected in October 2018 at a depth of -20 m off the Nansha Islands, Hainan Province, China. The fresh sample was immediately frozen. The animal material was identified by Prof. X.-B. Li (Hainan University). A voucher specimen (No. 18-NS-10) was deposited at the Institute of Tropical Bioscience and Biotechnology, Chinese Academy of Tropical Agricultural Sciences.

3.3. Extraction and Isolation

The frozen soft coral *S. crassocaule* (84.0 g, dry weight) was chopped into pieces and extracted with EtOH after sonication at room temperature (5×1.5 L). A brown residue was yielded after the organic extract was evaporated in vacuo and then partitioned between EtOAc and water. The EtOAc phase was evaporated in vacuo to yield a deep brown residue (8.0 g), which was then fractionated using gradient silica gel column chromatography (silica gel CC) (300–400 mesh) with $0 \rightarrow 100\%$ EtOAc in petroleum ether (PE), resulting in twenty-one fractions (A–U). Fraction U (814.0 mg) was separated into seven subfractions, U1–U7, using Sephadex LH-20 column chromatography (Sephadex LH-20

CC) eluted with 100% MeOH. Fraction U4 (242.0 mg) was separated using silica gel CC eluted with CH₂Cl₂/MeOH (60:1, 40:1) and subsequently purified using semi-preparative HPLC eluted with 75% aqueous MeOH (flow rate, 3.0 mL/min) to obtain compound **1** (1.4 mg, *t_R* = 15.0 min). Fractions S (1.8 g), T (120.0 mg), FG (384.0 mg), HI (405.0 mg) and M (707.0 mg) were all subjected to the same separation process of Sephadex LH-20 CC or silica gel CC as aforementioned to give a series of subfractions. Subfractions S5F (18.2 mg) and S7F2 (8.0 mg) were purified by semi-preparative HPLC eluted with 70% and 75% aqueous MeOH, respectively, to obtain compounds **3** (7.4 mg, *t_R* = 17.7 min) and **2** (3.7 mg, *t_R* = 15.9 min). Subfraction T2 (48.2 mg) was separated by silica gel CC using the ratios of CH₂Cl₂/MeOH (150:1, 90:1, 60:1) to yield compound **4** (2.7 mg). Subfractions T3B (11.5 mg), HI5E1 (9.4 mg) and M4D2 (5.6 mg) were purified by semi-preparative HPLC eluted with 70% (MeOH/H₂O), 70% (MeCN/H₂O) and 75% (MeOH/H₂O), respectively, to obtain compounds **5** (1.5 mg, *t_R* = 9.2 min), **6** (3.9 mg, *t_R* = 9.8 min) and **7** (3.2 mg, *t_R* = 13.7 min).

Sarcocrassolin A (**1**): White powder. $[\alpha]_D^{25} = -78$ (c 0.10, MeOH); UV (MeOH) λ_{\max} (log ϵ): 207 (3.22) nm; IR (KBr) ν_{\max} (cm⁻¹): 3418, 2958, 1638, 1462, 1377, 1071, 919. ¹H and ¹³C NMR data, see Tables 1 and 2; HRESIMS [M + Na]⁺ *m/z* 391.2820 (calcd. for C₂₂H₄₀O₄Na, 391.2819).

Sarcocrassolin B (**2**): Colorless crystals. M.p. 80–81 °C. $[\alpha]_D^{25} = -94$ (c 0.10, MeOH); UV (MeOH) λ_{\max} (log ϵ): 212 (3.34) nm; IR (KBr) ν_{\max} (cm⁻¹): 3421, 2960, 2929, 1602, 1457, 1377, 1267, 1126, 1086. ¹H NMR and ¹³C NMR data, see Tables 1 and 2; HRESIMS *m/z* 695.5211 [2M + Na]⁺ (calcd. for C₄₂H₇₂O₆Na, 695.5221).

Sarcocrassolin C (**3**): Colorless oil. $[\alpha]_D^{25} = -82$ (c 0.10, MeOH); UV (MeOH) λ_{\max} (log ϵ): 208 (3.25) nm; IR (KBr) ν_{\max} (cm⁻¹): 3431, 2958, 1632, 1461, 1376, 1085. ¹H and ¹³C NMR data, see Tables 1 and 2; HRESIMS [M + Na]⁺ *m/z* 391.2819 (calcd. for C₂₂H₄₀O₄Na, 391.2819).

Sarcocrassolin D (**4**): Colorless oil. $[\alpha]_D^{25} = -38$ (c 0.10, MeOH); UV (MeOH) λ_{\max} (log ϵ): 207 (3.15) nm; IR (KBr) ν_{\max} (cm⁻¹): 3430, 2960, 1649, 1461, 1375, 1080. ¹H and ¹³C NMR data, see Tables 1 and 2; HRESIMS [2M + Na]⁺ *m/z* 731.5432 (calcd. for C₄₂H₇₆O₈Na, 731.5432).

Sarcocrassolin E (**5**): Colorless oil. $[\alpha]_D^{25} = +6$ (c 0.10, MeOH); UV (MeOH) λ_{\max} (log ϵ): 209 (3.12) nm; IR (KBr) ν_{\max} (cm⁻¹): 3393, 2962, 1650, 1589, 1461, 1377, 1087. ¹H and ¹³C NMR data, see Tables 1 and 2; HRESIMS [M + Na]⁺ *m/z* 345.2398 (calcd. for C₂₀H₃₄O₃Na, 345.2400).

Sarcocrassolin F (**6**): Colorless oil. $[\alpha]_D^{25} = -75$ (c 0.10, MeOH); UV (MeOH) λ_{\max} (log ϵ): 213 (3.20) nm; IR (KBr) ν_{\max} (cm⁻¹): 3444, 2958, 1633, 1461, 1094. ¹H and ¹³C NMR data, see Tables 1 and 2; HRESIMS [M + Na]⁺ *m/z* 359.2557 (calcd. for C₂₁H₃₆O₃Na, 359.2557).

3.4. X-ray Crystallographic Analysis

The solvent methanol/H₂O (20:1) was used to create an acceptable crystal of compound **2** (0.15 × 0.12 × 0.1 mm³) at ambient temperature. The crystallographic data were collected at 170 K on a diffractometer Rigaku Oxford Diffraction Supernova Dual Source, Cu at Zero, equipped with an AtlasS2 CCD using Cu K α radiation ($\lambda = 1.54184$ Å) by using a ω scan mode. CrysAlisPro (version: 1.171.38.41) was used to process the data, and the structures were solved using direct methods with the SHELXT structure solution program via intrinsic phasing algorithm using Olex2 software (version: 1.5). The non-hydrogen atoms in the trial structure were detected and then refined anisotropically with SHELXL-2018 using a full-matrix least-squares program based on F^2 ; F^2 was used to obtain the weighted *R* factor, *wR* and goodness-of-fit *S* values. The placements of the hydrogen atoms were fixed geometrically at the calculated distances and permitted to ride on the parent atoms. Detailed crystallographic data are provided in the Supplementary Materials (Table S11) and have been deposited at the Cambridge Crystallographic Data Centre for inspection (deposition numbers: CCDC 2291468 for **2**).

Crystal data for compound **2**: C₂₁H₃₇O_{3.5}, *M* = 345.50, orthorhombic system, space group P2₁2₁2₁/c (no. 19), *a* = 9.5531(6) Å, *b* = 15.2772(15) Å, *c* = 28.949(5) Å, $\beta = 90^\circ$,

$V = 4224.9(8) \text{ \AA}^3$, $Z = 8$, $T = 169.99(10) \text{ K}$, $\mu(\text{Cu K}\alpha) = 0.564 \text{ mm}^{-1}$, $D_{\text{calc}} = 1.086 \text{ g/cm}^3$, 16,223 reflections measured ($8.416^\circ \leq 2\Theta \leq 147.908^\circ$), 8320 unique ($R_{\text{int}} = 0.1057$, $R_{\text{sigma}} = 0.2540$) which were used in all calculations. The final R_1 was 0.0784 ($I > 2\sigma(I)$), and wR_2 was 0.2254 (all data).

3.5. Computational Details

The torsional sampling (MCMM) method and the OPLS_2005 force field were used for carrying out a conformational search inside a 21 kJ/mol energy window. The conformers were reoptimized using the IEFPCM solvent model for chloroform at the B3LYP/6-31G(d) level for conformers over 1% Boltzmann populations. The reoptimized geometries' position at the energy minima was further verified by frequency analysis. Then, as advised for DP4+, NMR calculations were carried out at the PCM/mPW1PW91/6-311+G(d,p) level. The GIAO method was used to compute NMR shielding constants. After obtaining a Boltzmann distribution for each stereoisomer, shielding constants were averaged and correlated with the experimental results.

3.6. Cytotoxic Detection

The cytotoxic activity bioassay of all the abovementioned compounds was carried out as described in our previous paper [25]. Cisplatin was used as a positive control.

3.7. Anti-Inflammatory Assay

In the bioassay for anti-inflammation, all the abovementioned compounds were assayed for the inhibition of NO released in lipopolysaccharide-stimulated RAW264.7 cells (bought from the Stem Cell Bank of the Chinese Academy of Sciences) by the Griess method [26]. The mouse macrophage cells were cultured in 96-well plates at a concentration of 5×10^4 cells per mL (100 μL each well) in a humidified incubator of 5% CO_2 at 37°C for 24 h. The transfected cells were then stimulated using LPS (50 μL , 500 ng/mL) for 24 h after being treated with 50 μL solution of the tested compound at different concentrations (100.0, 50.0, 25.0, 12.5 μM) for 1 h. Then, 100 μL of supernatants were taken from each well, and 100 μL of Griess reagent (40 mg/mL) was added into a new 96-well plate. Finally, using a microplate reader, the absorbance of each well was measured at the wavelength of 540 nm. The IC_{50} was calculated using GraphPad Prism 9.0. The positive control employed was quercetin. The cytotoxicity of compounds against RAW264.7 cells was determined by the MTT method.

4. Conclusions

In conclusion, six uncommon capnosane-type macrocyclic diterpenes, sarcocrassinolins A–F (1–6), and one related known analog pavidolide D (7) were isolated from the soft coral *S. crassocaule* collected off the Nansha Islands. Due to the presence of a highly flexible macrocycle, the configuration assignments of capnosane-type macrocyclic diterpenes are still confronted with huge challenges. In our continuing efforts, the absolute configuration of compound 2 was assigned based on an X-ray crystallography study, and the relative configurations of the remaining compounds were established through QM-NMR using DP4+ probability analysis. Despite the fact that the soft coral *S. crassocaule* has been acknowledged as a major source of cembrane-type diterpenes, the capnosane-type macrocyclic diterpenes have not been previously reported. This is the first time that capnosane-type macrocyclic diterpenes were described in the soft coral *S. crassocaule*. Consequently, the soft coral *S. crassocaule* could be a potential source of structurally diverse capnosane-type macrocyclic diterpenes. In anti-inflammatory testing, all isolated compounds were assayed for the inhibitory activity on NO release in LPS-induced RAW264.7 cells. Sarcocrassinolin D (4) and sarcocrassinolin E (5) exhibited weak inhibitory effects. Furthermore, all compounds were tested for cytotoxicity. Unfortunately, none of the compounds demonstrated notable activity.

Supplementary Materials: The following supporting information can be downloaded at: <https://www.mdpi.com/article/10.3390/md21120645/s1>. Figures S1–S56: 1D, 2D NMR, MS, UV and IR spectra of compounds 1–7, Figures S57–S60: Structures of isomers of compounds 3–6, Tables S1–S10 and Figure S61: QM-NMR data, Table S11: Crystal data and structure refinement for compound 2.

Author Contributions: H.P. and Y.Z.: writing—original draft, isolation and structure elucidation. H.W., W.C., H.C. and F.Z.: assisting with the experiments. Y.Z.: collecting samples. Y.Z., H.D. and X.W.: writing—review and editing, supervision, funding acquisition. All authors have read and agreed to the published version of the manuscript.

Funding: This research work was financially supported by the Key Research and Development Project of Hainan Province (ZDYF2021SHFZ107), National Natural Science Foundation of China (41776093) and the Financial Fund of the Ministry of Agriculture and Rural Affairs, China (NFZX2021).

Institutional Review Board Statement: Not applicable.

Data Availability Statement: The authors declare that all relevant data supporting the results of this study are available within the article and its Supplementary Materials file, or from the corresponding authors upon request.

Conflicts of Interest: The authors declare no conflict of interest.

References

1. Yang, B.; Zhou, X.F.; Lin, X.P.; Liu, J.; Peng, Y.; Yang, X.W.; Liu, Y.H. Cembrane diterpenes chemistry and biological properties. *Curr. Org. Chem.* **2012**, *16*, 1512–1539. [[CrossRef](#)]
2. Dauben, W.G.; Thiessen, W.E.; Resnick, P.R. Cembrene, a fourteen-membered ring diterpene hydrocarbon. *J. Org. Chem.* **1965**, *30*, 1693–1698. [[CrossRef](#)]
3. Du, Y.Q.; Chen, J.; Wu, M.J.; Zhang, H.Y.; Liang, L.F.; Guo, Y.W. Uncommon capnosane diterpenes with neuroprotective potential from South China Sea soft coral *Sarcophyton boettgeri*. *Mar. Drugs* **2022**, *20*, 602. [[CrossRef](#)] [[PubMed](#)]
4. Kobayashi, M.; Nakano, E. Stereochemical course of the transannular cyclization, in chloroform, of epoxycebranoids derived from the geometrical isomers of (14S)-14-hydroxy-1,3,7,11-cembratetraenes. *J. Org. Chem.* **1990**, *55*, 1947–1951. [[CrossRef](#)]
5. Li, Y.; Pattenden, G. Perspectives on the structural and biosynthetic interrelationships between oxygenated furanocembranoids and their polycyclic congeners found in corals. *Nat. Prod. Rep.* **2011**, *28*, 1269–1310. [[CrossRef](#)]
6. Liu, Z.; Cheng, W.; Liu, D.; van Ofwegen, L.; Proksch, P.; Lin, W.H. Capnosane-type cembranoids from the soft coral *Sarcophyton trocheliophorum* with antibacterial effects. *Tetrahedron* **2014**, *70*, 8703–8713. [[CrossRef](#)]
7. Chen, W.T.; Yao, L.G.; Li, X.W.; Guo, Y.W. Sarcophytrols A–C, new capnosane diterpenoids from the South China Sea soft coral *Sarcophyton trocheliophorum*. *Tetrahedron Lett.* **2015**, *56*, 1348–1352. [[CrossRef](#)]
8. Liang, L.F.; Kurtán, T.; Mándi, A.; Gao, L.X.; Li, J.; Zhang, W.; Guo, Y.W. Sarsolenane and capnosane diterpenes from the Hainan soft coral *Sarcophyton trocheliophorum* marenzeller as PTP1B inhibitors. *Eur. J. Org. Chem.* **2014**, *2014*, 1841–1847. [[CrossRef](#)]
9. Song, Y.T.; Yu, D.D.; Su, M.Z.; Luo, H.; Cao, J.G.; Liang, L.F.; Yang, F.; Guo, Y.W. Structurally diverse diterpenes from the South China Sea soft coral *Sarcophyton trocheliophorum*. *Mar. Drugs* **2023**, *21*, 69. [[CrossRef](#)]
10. Tseng, W.R.; Ahmed, A.F.; Huang, C.Y.; Tsai, Y.Y.; Tai, C.J.; Orfali, R.S.; Hwang, T.L.; Wang, Y.H.; Dai, C.F.; Sheu, J.H. Bioactive capnosanes and cembranes from the soft coral *Klyxum flaccidum*. *Mar. Drugs* **2019**, *17*, 461. [[CrossRef](#)]
11. Lai, D.; Geng, Z.F.; Deng, Z.W.; van Ofwegen, L.; Proksch, P.; Lin, W.H. Cembranoids from the soft coral *Simularia rigida* with antifouling activities. *J. Agric. Food Chem.* **2013**, *61*, 4585–4592. [[CrossRef](#)] [[PubMed](#)]
12. Ye, F.; Zhu, Z.D.; Gu, Y.C.; Li, J.; Zhu, W.L.; Guo, Y.W. Further new diterpenoids as PTP1B inhibitors from the Xisha soft coral *Simularia polydactyla*. *Mar. Drugs* **2018**, *16*, 103. [[CrossRef](#)] [[PubMed](#)]
13. Bu, Q.; Yang, M.; Yan, X.Y.; Li, S.W.; Ge, Z.Y.; Zhang, L.; Yao, L.G.; Guo, Y.W.; Liang, L.F. Mililatensols A–C, new records of sarsolenane and capnosane diterpenes from soft coral *Sarcophyton mililatensis*. *Mar. Drugs* **2022**, *20*, 566. [[CrossRef](#)]
14. Shen, S.; Zhu, H.J.; Chen, D.W.; Liu, D.; van Ofwegen, L.; Proksch, P.; Lin, W.H. Pavidolides A–E, new cembranoids from the soft coral *Simularia pavidula*. *Tetrahedron Lett.* **2012**, *53*, 5759–5762. [[CrossRef](#)]
15. Xi, Z.F.; Bie, W.; Chen, W.; Liu, D.; van Ofwegen, L.; Proksch, P.; Lin, W.H. Sarcophytolides B–E, new cembranoids from the soft coral *Sarcophyton elegans*. *Mar. Drugs* **2013**, *11*, 3186–3196. [[CrossRef](#)] [[PubMed](#)]
16. Zhang, Q.; Li, X.W.; Yao, L.G.; Wu, B.; Guo, Y.W. Three new capnosane-type diterpenoids from the South China Sea soft coral *Lobophytum* sp. *Fitoterapia* **2019**, *133*, 70–74. [[CrossRef](#)]
17. Zhang, M.; Long, K.H.; Shi, S.H.; Mak, T.C.W. A novel diterpenolide from the soft coral *Sarcophyton solidum*. *J. Nat. Prod.* **1992**, *55*, 1672–1675. [[CrossRef](#)]
18. Bowden, B.F.; Coll, J.C.; Gulbis, J.M.; Mackay, M.F.; Willis, R.H. Studies of Australian soft corals. XXXVIII. Structure determination of several diterpenes derived from a cespitularia species (*coelenterata*, *octocorallia*, *xeniidae*). *Aust. J. Chem.* **1986**, *39*, 803–812. [[CrossRef](#)]

19. D'Ambrosio, M.; Guerriero, A.; Pietra, F. Novel cembranolides (coralloidolide D and E) and a 3,7-cyclized cembranolide (coralloidolide C) from the mediterranean coral *Alcyonium coralloides*. *Helv. Chim. Acta.* **1989**, *72*, 1590–1596. [[CrossRef](#)]
20. Zhang, D.; Li, Y.Y.; Li, X.L.; Han, X.; Wang, Z.; Li, G.Q. A new capnosane-type diterpenoid from the South China sea soft coral *Lobophytum pauciflorum*. *Nat. Prod. Res.* **2024**, *38*, 97–102. [[CrossRef](#)]
21. Li, J.; Huan, X.J.; Wu, M.J.; Chen, Z.H.; Chen, B.; Miao, Z.H.; Guo, Y.W.; Li, X.W. Chemical constituents from the South China sea soft coral *Sinularia humilis*. *Nat. Prod. Res.* **2022**, *36*, 3324–3330. [[CrossRef](#)] [[PubMed](#)]
22. Elkhawas, Y.A.; Elissawy, A.M.; Elnaggar, M.S.; Mostafa, N.M.; Al-Sayed, E.; Bishr, M.M.; Singab, A.N.B.; Salama, O.M. Chemical diversity in species belonging to soft coral genus *Sarcophyton* and its impact on biological activity: A review. *Mar. Drugs* **2020**, *18*, 41. [[CrossRef](#)] [[PubMed](#)]
23. Rodrigues, I.G.; Miguel, M.G.; Mnif, W. A brief review on new naturally occurring cembranoid diterpene derivatives from the soft corals of the genera *Sarcophyton*, *Sinularia*, and *Lobophytum* since 2016. *Molecules* **2019**, *24*, 781. [[CrossRef](#)] [[PubMed](#)]
24. Li, J.F.; Zeng, Y.B.; Li, W.S.; Luo, H.; Zhang, H.Y.; Guo, Y.W. Xishaglaucumins A–J, new cembranoids with anti-inflammatory activities from the South China Sea soft coral *Sarcophyton glaucum*. *Chin. J. Chem.* **2022**, *40*, 79–90. [[CrossRef](#)]
25. Zeng, Y.B.; Wang, Z.; Chang, W.J.; Zhao, W.B.; Wang, H.; Chen, H.Q.; Dai, H.F.; Lv, F. New azaphilones from the marine-derived fungus *Penicillium sclerotiorum* E23Y-1A with their anti-inflammatory and antitumor activities. *Mar. Drugs* **2023**, *21*, 75. [[CrossRef](#)]
26. Chen, H.Q.; Guo, D.S.; Wang, H.; Cai, C.H.; Yuan, J.Z.; Dai, H.F.; Yang, L.; Mei, W.L. Sesquiterpenoids and bibenzyl derivative from *Dendrobium hercoglossum*. *Fitoterapia* **2024**, *172*, 105748. [[CrossRef](#)]

Disclaimer/Publisher's Note: The statements, opinions and data contained in all publications are solely those of the individual author(s) and contributor(s) and not of MDPI and/or the editor(s). MDPI and/or the editor(s) disclaim responsibility for any injury to people or property resulting from any ideas, methods, instructions or products referred to in the content.